Linear dynamics of free-piston Stirling engines

R W Redlich, BS, MS, PhD
Department of Electrical and Computer Engineering, Ohio University, Athens, Ohio

D M Berchowitz, BSc, MSc
Sunpower Incorporated, Athens, Ohio

The free-piston Stirling engine (FPSE) is a heat driven mechanical oscillator from which power can be extracted. Linear dynamics is applied here in order to obtain: a stability criterion, a means for determining the oscillation frequency, relative amplitudes of the dynamic components, effects of friction on starting and the locus of the roots of the system determinant. Three common configurations of these engines are investigated.

NOTATION

A	cylinder area
A_d	displacer rod area
A_p	piston area
D	damping constant
F_p	pressure forces
F_{sl}	sliding friction force
j	$\sqrt{-1}$
K	spring constant
LHP	left half plane
m	component mass
m_t	total mass of gas
p	pressure
p_d	gas spring pressure
p_o	mean cycle pressure
P	power
Q	stored energy/energy dissipated per cycle
R	gas constant
RHP	right half plane
s	Laplace transform variable
t	time
T_c	cold end temperature
T_h	hot end temperature
T_r	regenerator effective temperature
V	phasor, volume
V_c	compression space volume
V_e	expansion space volume
V_h	heater volume
V_k	cooler volume
V_r	regenerator void volume
V_C	compression space swept volume
V_E	expansion space swept volume
W	work
x	displacement
$\dot{x}$	velocity
$\ddot{x}$	acceleration
$\hat{x}$	transformed displacement
X	amplitude, phasor
ϕ	phase angle, piston to displacer
θ	phasor angle
ω	frequency (rad/s)

Subscripts

c	casing, operating condition
d	displacer
p	piston
1, 2	roots

The MS was received on 26 June 1984 and was accepted for publication on 25 March 1985.

1 INTRODUCTION

Free-piston engines use variations of working gas pressure to drive mechanically unconstrained reciprocating elements. Stirling cycle free-piston engines are driven by the Stirling thermodynamic cycle which is characterized by an externally heated device containing working gas that is continuously re-used in a regenerative, reversible cycle (**1**). The ideal cycle is described by two isothermal processes connected by two constant volume processes. Heat removed during the constant volume cooling process is internally transferred to the constant volume heating process by mutual use of a thermal storage medium called the regenerator. Since the ideal cycle is reversible, the ideal efficiency is that of Carnot.

Potential advantages of the free-piston Stirling engine are: high efficiency, few moving parts, multi-fuel capability and the possibility of generating power over a wide range of source temperatures. In addition the engine may be hermetically sealed and is therefore not subject to problems caused by dirt ingress or leakage. One typical configuration of a free-piston Stirling engine driving a linear alternator is shown in Fig. 1. Other applications are water pumps, and, if the load device is a second Stirling cycle operating as a heat pump, domestic heat pumps, food freezers and natural gas liquefiers (**1**–**5**).

The purpose of this paper is to describe the dynamic operation of these machines, and, in particular, to obtain an understanding of the requirements for oscillation and the general behaviour under load.

2 LINEAR MODEL

Referring to Fig. 1, piston motion causes changes in working gas pressure, p, that excite motion of the displacer which transfers working gas between the hot and cold spaces thus changing p and hence also the force on the piston. Oscillation occurs under proper conditions

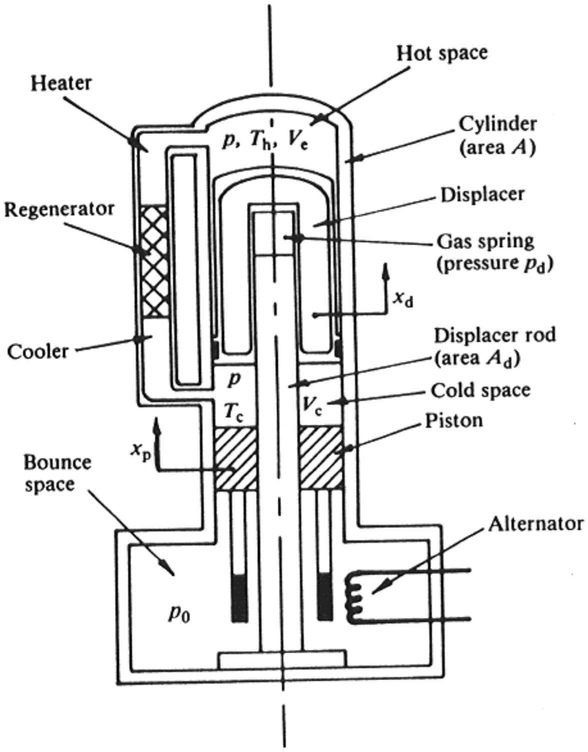

Fig. 1 Free-piston Stirling engine

and power may be removed by, for example, a reciprocating electric generator (linear alternator) as shown.

Consider firstly the displacer. The equation of motion may be written as follows:

$$m_d \ddot{x}_d = -D_d \dot{x}_d + A_d(p_d - p) \quad (1)$$

where damping is due to viscous forces on the moving gas. In general there is a further coupling to the piston velocity, because piston motion causes a pressure drop across the heat exchangers. In the interests of simplicity, this coupling is ignored here as it does not significantly alter the conclusions of the linear analysis. However this effect can be included by straightforward extension of the analysis presented here. Other incidental irreversibilities such as gas spring hysteresis have been partly accounted for in D_d and D_p.

Linearizing equation (1):

$$m_d \ddot{x}_d = -D_d \dot{x}_d + A_d\left[\left(\frac{\partial p_d}{\partial x_d} - \frac{\partial p}{\partial x_d}\right)x_d - \frac{\partial p}{\partial x_p} x_p\right] \quad (2)$$

Taking the Laplace transform and writing K_d for the coefficient of x_d in (2) gives:

$$(m_d s^2 + D_d s + K_d)\hat{x}_d = -\left(\frac{\partial p}{\partial x_p} A_d\right)\hat{x}_p + (\text{initial conditions})_d \quad (3)$$

The term (initial conditions)$_d$ is of the form $(as + b)$, where a and b depend on initial values of x_d and x_p. Equation (3) can be recast in terms of quantities ω_d, Q_d and α_p, defined as follows:

$$\omega_d = \text{undamped resonance frequency} = \sqrt{(K_d/m_d)} \quad (3a)$$

$$Q_d = (\text{stored displacer energy/energy loss per cycle at } \omega_d) = \frac{\omega_d}{2\pi}\frac{m_d}{D_d} \quad (3b)$$

$$\alpha_p = A_d \frac{\partial p}{\partial x_p} \quad (3c)$$

with these definitions equation (3) becomes:

$$m_d\left(s^2 + \frac{\omega_d}{2\pi Q_d} s + \omega_d^2\right)\hat{x}_d + \alpha_p \hat{x}_p = (\text{initial conditions})_d \quad (4)$$

With the further definition:

$$T_d(s) = m_d\left(s^2 + \frac{\omega_d}{2\pi Q_d} s + \omega_d^2\right) \quad (5)$$

equation (4) becomes:

$$T_d(s)\hat{x}_d + \alpha_p \hat{x}_p = (\text{initial conditions})_d \quad (6)$$

To obtain the linearized equation of piston motion, it is first noted that the linearized unbalanced pressure force on the piston, F_p, is given by:

$$F_p = -(A - A_d)\left(\frac{\partial p}{\partial x_d} x_d + \frac{\partial p}{\partial x_p} x_p\right) \quad (7)$$

The second term on the right of equation (7) is the piston gas spring constant, K_p, that is,

$$K_p = (A - A_d)\frac{\partial p}{\partial x_p} \quad (8)$$

The first term on the right of equation (7) is a thermodynamic coupling between piston force and displacer motion. The piston is also subjected to a damping force $-D_p \dot{x}_p$ from the electric generator (or other useful load) plus incidental irreversibilities. Thus the Laplace transformed equation of piston motion is:

$$(m_p s^2 + D_p s + K_p)\hat{x}_p + (A - A_d)\frac{\partial p}{\partial x_d}\hat{x}_d = (\text{initial conditions})_p \quad (9)$$

With the further definitions:

$$\omega_p = \sqrt{(K_p/m_p)} \quad \text{(undamped piston resonant frequency)} \quad (9a)$$

$$Q_p = \frac{\omega_p}{2\pi}\frac{m_p}{D_p} \quad \text{(stored piston energy/energy loss per cycle at } \omega_p) \quad (9b)$$

$$\alpha_T = (A - A_d)\frac{\partial p}{\partial x_d} \quad \text{(thermal coupling between displacer motion and piston force)} \quad (9c)$$

$$T_p(s) = m_p\left(s^2 + \frac{\omega_p}{2\pi Q_p} s + \omega_p^2\right) \quad (9d)$$

the equations of motion of displacer and piston are:

$$T_d(s)\hat{x}_d + \alpha_p \hat{x}_p = (\text{initial conditions})_d \quad (6)$$

$$\alpha_T \hat{x}_d + T_p(s)\hat{x}_p = (\text{initial conditions})_p \quad (10)$$

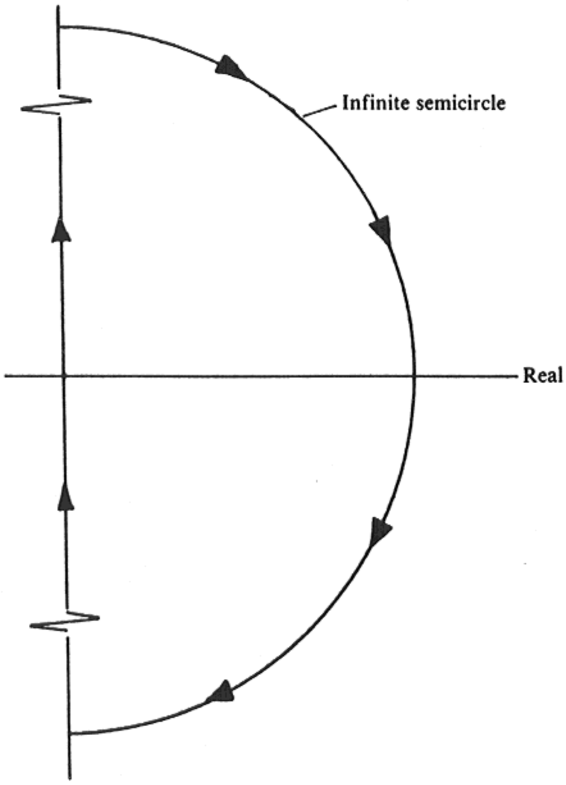

Fig. 2 Bromwich contour

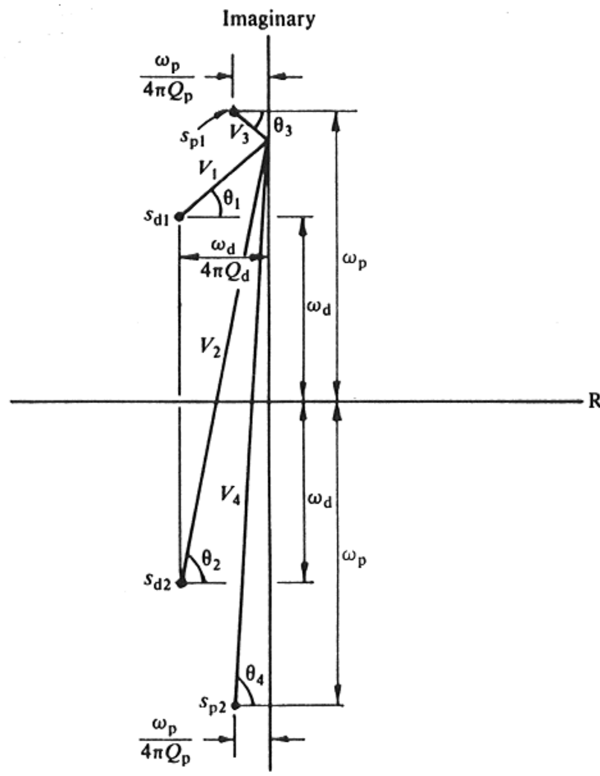

Fig. 3 Zero locations in the complex plane

The nature of the solutions for $x_d(t)$ and $x_p(t)$ will be determined by the location in the complex plane of the four roots of

$$\begin{vmatrix} T_d(s) & \alpha_p \\ \alpha_T & T_p(s) \end{vmatrix} = 0 \tag{11}$$

or

$$T_d(s)T_p(s) - \alpha_p \alpha_T = 0 \tag{12}$$

A necessary condition for oscillation is the presence of at least two roots in the RHP. Whether such roots exist can be determined by examining a map in the complex plane of the left side of equation (12) as s traces the Bromwich contour (Fig. 2) in a clockwise sense. Since the left side of equation (12) has no RHP poles the number of clockwise encirclements of the origin by the map is equal to the number of RHP roots of equation (12) (6).

Since α_T is a negative quantity in practice (pressure decreases as displacer moves up), an equivalent statement is that the number of RHP roots of equation (12) is equal to the number of encirclements of the point $-|\alpha_p \alpha_T| + j(0)$ by a map of $T_d(s)T_p(s)$ as s traces the Bromwich contour. $T_d(s)T_p(s)$ is of fourth order, and it can be factored into:

$$T_d(s)T_p(s) = (s - s_{d_1})(s - s_{d_2})(s - s_{p_1})(s - s_{p_2}) \tag{13}$$

where s_{d_1}, s_{d_2} are the roots of $T_d(s) = 0$ and s_{p_1}, s_{p_2} are the roots of $T_p(s) = 0$.

From the definitions of $T_d(s)$, $T_p(s)$, and the quadratic formula:

$$s_{d_1}, s_{d_2} = \omega_d \left\{ -\frac{1}{4\pi Q_d} \pm j \sqrt{\left[1 - \left(\frac{1}{4\pi Q_d}\right)^2\right]} \right\} \tag{14}$$

$$s_{p_1}, s_{p_2} = \omega_p \left\{ -\frac{1}{4\pi Q_p} \pm j \sqrt{\left[1 - \left(\frac{1}{4\pi Q_p}\right)^2\right]} \right\} \tag{15}$$

In practical machines, Q_d and Q_p usually exceed 1.0, and to the first order in $1/4\pi Q$;

$$s_{d_1}, s_{d_2} = \omega_d \left(-\frac{1}{4\pi Q_d} \pm j \right) \tag{16}$$

$$s_{p_1}, s_{p_2} = \omega_p \left(-\frac{1}{4\pi Q_p} \pm j \right) \tag{17}$$

Figure 3 shows schematically the location of s_{d_1}, s_{d_2}, s_{p_1} and s_{p_2} in the complex plane. In Fig. 3, the factors of $T_d(s)T_p(s)$ are represented by the phasors V_1, V_2, V_3, V_4 if s is on the imaginary axis.

To begin the mapping of $T_d(s)T_p(s)$, traversal of the Bromwich contour can be started at $s = 0$, for which point $(\theta_1 + \theta_2 + \theta_3 + \theta_4) = 0$, hence $T_d(0)T_p(0)$ is real and positive. As s progresses up the imaginary axis, angles θ_2 and θ_4 increase, while the negative angles θ_1, θ_3 decrease in magnitude and eventually become positive. Thus the map begins on the real axis and moves into the first quadrant. As $s \to j(\infty)$, $(\theta_1 + \theta_2 + \theta_3 + \theta_4) \to 2\pi$. Therefore the map circles the origin counterclockwise and returns to the real axis at $+\infty$.

The next section of the contour to be traversed is an infinite RHP semicircle. As s moves clockwise on this section from $+j\infty$ to $-j\infty$, $(\theta_1 + \theta_2 + \theta_3 + \theta_4)$

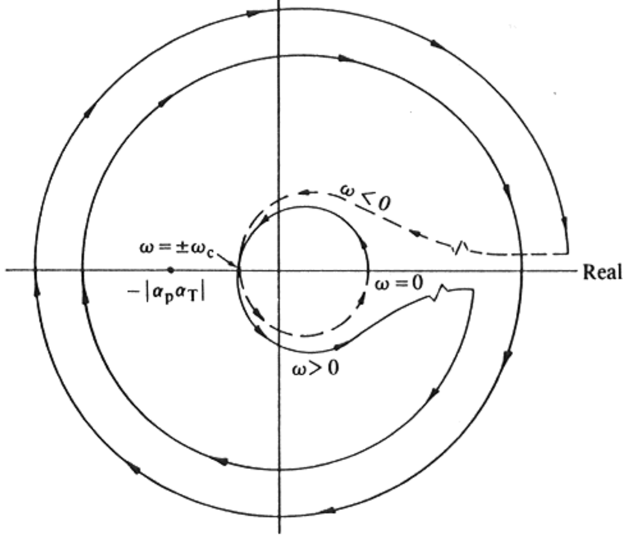

Fig. 4a Two RHP roots

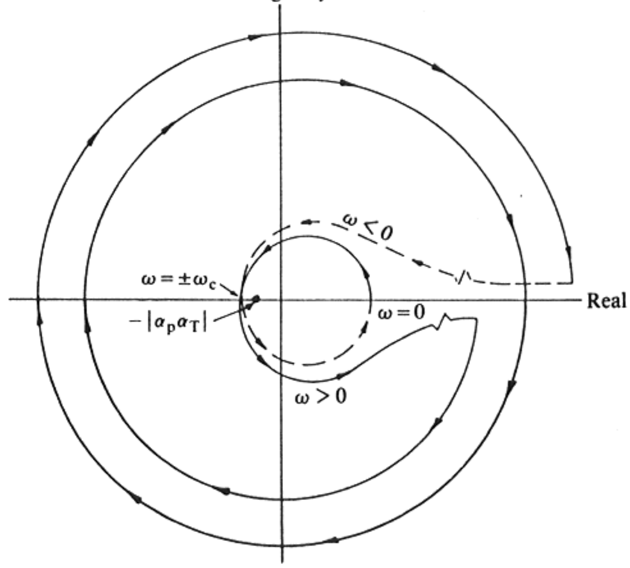

Fig. 4b No RHP roots

decreases from 2π to -2π, and the map of $T_d(s)T_p(s)$ is two circles of infinite radius, traversed clockwise.

The last section of the contour is the negative imaginary axis from $-j\infty$ to the origin, for which the map is the complex conjugate of that for the positive imaginary axis.

Maps of $T_d(s)T_p(s)$ are shown in Figs. 4a and 4b, for cases where there are two RHP roots of equation (12) and no RHP roots, respectively. Figure 4a shows two clockwise encirclements of $-|\alpha_p \alpha_T|$, while Fig. 4b shows two clockwise and two counterclockwise encirclements, or no net encirclements, hence no RHP roots of equation (12).

The frequency ω_c in Figs. 4a and 4b is that for which

$$\theta_1(\omega_c) + \theta_2(\omega_c) + \theta_3(\omega_c) + \theta_4(\omega_c) = \pi \tag{18}$$

From Figs. 4a and 4b, a necessary condition for oscillation is then

$$|T_d(j\omega_c)T_p(j\omega_c)| < |\alpha_p \alpha_T| \tag{19}$$

From Fig. 3 it is clear that ω_c lies between ω_p and ω_d, and approximately satisfies the condition

$$\theta_1(\omega_c) = -\theta_3(\omega_c) \tag{20}$$

In the borderline case, characterized by

$$T_d(j\omega_c)T_p(j\omega_c) + |\alpha_p \alpha_T| = 0 \tag{21}$$

equation (12) has roots at $\pm j\omega_c$.

It will be shown later that if equation (12) has two RHP roots, they are a complex conjugate pair rather than two positive real roots. This is of practical significance since the dynamic consequences of RHP real roots would disqualify the machine as a practical oscillator.

If equation (12) has a conjugate pair of RHP roots, the remaining two roots are LHP, and their dynamic consequences eventually disappear.

If a conjugate pair of RHP roots of equation (12) does exist, the machine will oscillate with exponentially increasing amplitude until limited by non-linearities, which can be artificially introduced by feedback mechanisms, or be inherent in the internal gas dynamics. Without non-linearities, oscillation will build up to mechanical limits.

The oscillation criterion (19) can be expressed in a practical form involving engine parameters. The first step in doing so is to determine ω_c, using equation (18). For practical cases, $\theta_2 + \theta_4 \approx \pi$ at $\omega = \omega_c$, and ω_c is located by requiring $\theta_1 = -\theta_3$, which leads to:

$$\omega_c \approx \frac{\omega_d \omega_p (Q_p + Q_d)}{\omega_p Q_d + \omega_d Q_p} \tag{22}$$

If $Q_d \gg Q_p$, $\omega_c \approx \omega_d$; and if $Q_p \gg Q_d$, $\omega_c \approx \omega_p$. In general, it follows from equation (22) that ω_c is closer to the resonance frequency associated with the higher Q. A further observation is that since Q_p changes with load, the operating frequency is, in general, a function of load. The engine may be made to operate at a constant frequency over a wide range in load by arranging $\omega_d = \omega_p$ in which case ω_c is independent of Q_d and Q_p. An alternative way of achieving near constant frequency with load variations is to ensure that $Q_d \gg Q_p$ over the full range of load, so that $\omega_c \approx \omega_d$ regardless of Q_p.

In terms of ω_c, ω_d and ω_c, the oscillation criterion (19) becomes:

$$m_p m_d (\omega_c + \omega_p)(\omega_c + \omega_d)\left[(\omega_c - \omega_d)^2 + \frac{\omega_d^2}{(4\pi Q_d)^2}\right]^{1/2} \cdot \left[(\omega_c - \omega_p)^2 + \frac{\omega_p^2}{(4\pi Q_p)^2}\right]^{1/2} < |\alpha_p \alpha_T| \tag{23}$$

which is a general criterion for oscillation. For the special case $\omega_c = \omega_p = \omega_d$, equation (23) reduces to

$$\frac{m_p m_d \omega^4}{4\pi^2 Q_p Q_d} < |\alpha_p \alpha_T| \tag{23a}$$

3 ROOT LOCI

The locus of the roots of equation (12) as $|\alpha_p \alpha_T|$ varies can be inferred from equation (18) and the fact that the starting points of the root loci, for $|\alpha_p \alpha_T| = 0$, are the roots of $T_d(s) = 0$ and $T_p(s) = 0$, as given by equations

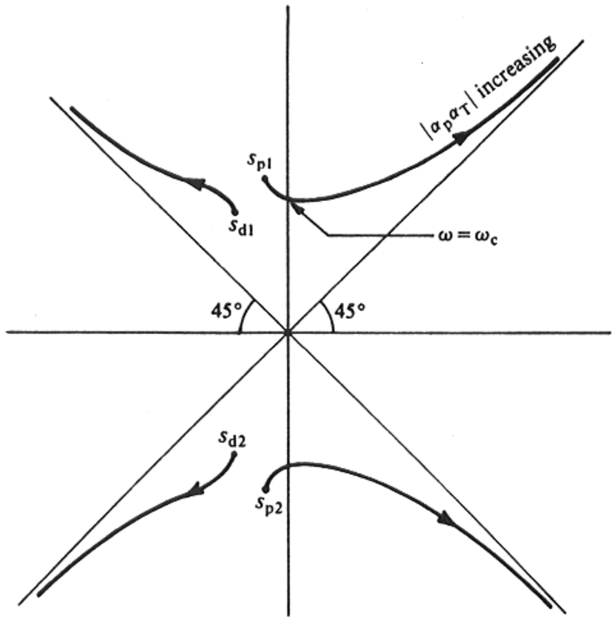

Fig. 5 Root locus with $|\alpha_p \alpha_T|$ as parameter

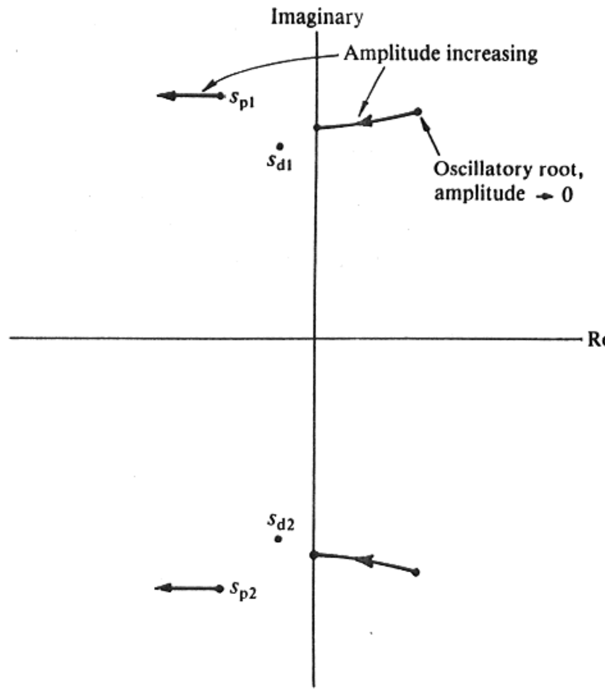

Fig. 6 Root locus for Q_p decreasing with increasing amplitude

(16) and (17). Figure 5 shows typical resulting loci for a case $Q_p > Q_d$.

As α_T increases (due to increase in hot end temperature, as will be shown later), one conjugate pair of roots moves from $\pm s_{p_1}$ toward the $j\omega$ axis, eventually reaching it at a value of $\alpha_T \alpha_p$ predicted by the stability criterion, whereupon oscillation begins. The other two roots are a conjugate pair in the LHP and are associated with dynamic evanescence.

In practice, oscillation amplitude is limited by nonlinearities, either artificially induced by means of closed loop mechanisms that control Q_p or Q_d in response to piston amplitude, or inherent in the working gas flow processes, or both. Their effect is to decrease the positive real part of the conjugate root pair associated with oscillation as amplitude increases, until the roots eventually reach the imaginary axis at an equilibrium amplitude, as illustrated in Fig. 6 for a situation where Q_p decreases with amplitude.

When equilibrium is reached, piston and displacer motion are expressible in complex form as:

$$x_d(t) = X_d e^{j\omega_c t} \tag{24}$$

$$x_p(t) = X_p e^{j\omega_c t} \tag{24a}$$

where X_d and X_p are complex amplitudes and the operation of taking the real part of the right hand sides is understood. X_d and X_p are not independent but are related by either equations (6) or (10), which are equivalent by virtue of equation (11) at $s = \pm j\omega_c$. Thus, from equation (6):

$$\frac{X_d}{X_p} = -\frac{\alpha_p}{T_d(j\omega_c)} \tag{25}$$

from which follows the stroke ratio and piston/displacer phase angle:

$$\left|\frac{X_d}{X_p}\right| = \frac{\alpha_p}{K_d}\left\{\left[1-\left(\frac{\omega_c}{\omega_d}\right)^2\right]^2 + \left[\frac{\omega_c}{\omega_d}\cdot\frac{1}{2\pi Q_d}\right]^2\right\}^{-1/2} \tag{26}$$

$$\phi = \tan^{-1}\left[\left(\frac{\omega_c}{\omega_d}\cdot\frac{1}{2\pi Q_d}\right)\Big/\left(\frac{\omega_c^2}{\omega_d^2}-1\right)\right] \tag{27}$$

For practical engines, ϕ is usually between 40° and 90°. For the special case $\omega_c \approx \omega_p = \omega_d$, $\phi = \pi/2$ and $|X_d/X_p| = (\alpha_p/\omega D_p)$.

At equilibrium, the average power taken from the piston by useful load and internal losses is balanced by the average power, P, supplied to the piston by the working gas. The latter is the time average of the product of pressure forces on the piston and piston velocity, or

$$P = \langle (K_p x_p - \alpha_T x_d)\dot{x}_p \rangle \tag{28}$$

where the brackets denote time average. However, $\langle x_p \dot{x}_p \rangle = 0$, $\dot{x}_p = j\omega X_p e^{j\omega t}$ and, in general, the time average of the product of two sinusoidal quantities described by phasors $\boldsymbol{A}$ and $\boldsymbol{B}$ is given by $(\boldsymbol{AB}^* + \boldsymbol{A}^*\boldsymbol{B})/4$ where $\boldsymbol{A}^*$ and $\boldsymbol{B}^*$ denote complex conjugates. Therefore,

$$P = -j\omega\frac{\alpha_T}{4}(X_d^* X_p - X_d X_p^*)$$

or

$$P = \frac{\omega|\alpha_T|}{2}\,\text{imag}\,(X_d X_p^*)$$

If $X_d/X_p = Re^{j\phi}$, R real and positive, then

$$P = \frac{\omega|\alpha_T|}{2}|X_d||X_p|\sin\phi \tag{29}$$

Power is maximized for $\phi = 90°$, which, from equations (27) and (22), occurs when $\omega_p = \omega_d$. However, in practical engines the efficiency usually improves at the lower values of ϕ owing to reduced gas flow losses through the heat exchangers.

From equations (29) and the results for stability, frequency, stroke ratio and phase angle, i.e. equations (22), (23), (26) and (27) respectively, it is possible to define an engine. The accuracy of the result for power is limited by extrapolation of the linear solutions to large amplitudes and, of course, the accuracy in determining α_p and α_T. For the purposes of preliminary design, simple isothermal thermodynamics has been found to return reasonable approximations for α_p and α_T.

4 SIMPLE THERMODYNAMICS FOR EVALUATING α_p AND α_T

α_p and α_T can be approximated from simple thermodynamics which assumes all the gas in the hot space is at temperature T_h and all the gas in the cold space at T_c (**1**, **2**, **7**). From the ideal gas law:

$$m_t = p(V_c/T_c + V_k/T_c + V_r/T_r + V_h/T_h + V_e/T_h)/R \quad (30)$$

where m_t is the invariant total mass of gas in the working space of the engine and p is the gas pressure which is assumed to be spatially constant but time variant. T_r is the effective gas temperature in the regenerator and is usually taken to be the log mean temperature difference (**7**):

$$T_r = (T_h - T_c)/\ln(T_h/T_c) \quad (31)$$

In equation (30), V_c and V_e are functions of x_d and x_p. Referring to Fig. 1, the following holds:

$$\frac{dV_e}{dx_d} = -A \quad (32)$$

$$\frac{\partial V_c}{\partial x_d} = (A - A_d) \quad (33)$$

$$\frac{\partial V_c}{\partial x_p} = -(A - A_d) \quad (34)$$

It can be shown that the average pressure, p_o, is approximately the pressure for which $V_c = V_C/2$ and $V_e = V_E/2$, thus,

$$p_o = m_t R\left[\frac{1}{T_c}\left(\frac{V_C}{2} + V_k\right) + \frac{V_r}{T_r} + \frac{1}{T_h}\left(\frac{V_E}{2} + V_h\right)\right]^{-1}$$

or defining

$$\frac{V_o}{T_o} = \frac{1}{T_c}\left(\frac{V_C}{2} + V_k\right) + \frac{V_r}{T_r} + \frac{1}{T_h}\left(\frac{V_E}{2} + V_h\right) \quad (35)$$

$$p_o = m_t R T_o/V_o \quad (36)$$

From equations (30), and (32–36) and assuming that m_t is constant, the following is obtained at $p = p_o$, $V_c = V_C/2$, $V_e = V_E/2$.

$$\frac{\partial p}{\partial x_d} = -p_o \frac{T_o}{V_o}\frac{A}{T_c}\left(1 - \frac{T_c}{T_h} - \frac{A_d}{A}\right) \quad (37)$$

$$\frac{\partial p}{\partial x_p} = p_o \frac{T_o}{V_o}\frac{A}{T_c}\left(1 - \frac{A_d}{A}\right) \quad (38)$$

From equations (37) and (38) and the definitions of α_p and α_T [equations (3c) and (9c)]:

$$\alpha_p = p_o \frac{T_o}{V_o}\frac{A_d}{T_c}(A - A_d) \quad (39)$$

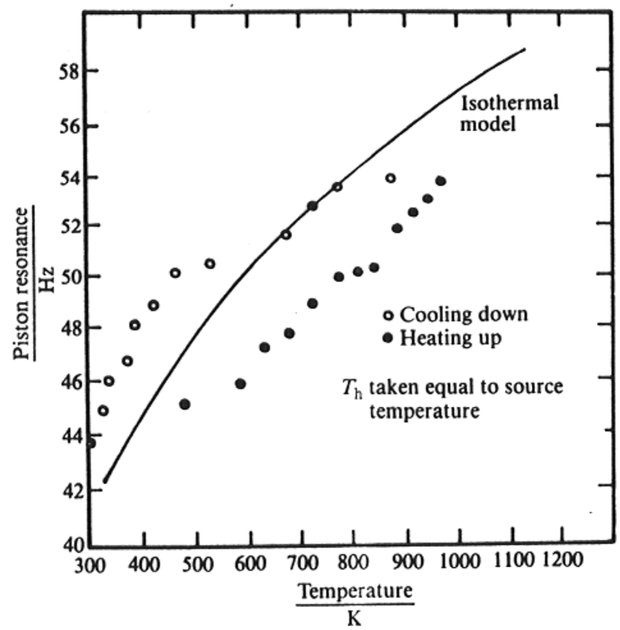

Fig. 7 Piston resonance versus temperature

$$\alpha_T = -p_o \frac{T_o}{V_o}\frac{A}{T_c}(A - A_d)\left(1 - \frac{T_c}{T_h} - \frac{A_d}{A}\right) \quad (40)$$

Noting that for bounce space pressures approximately constant, K_p, the piston spring constant is given by:

$$K_p = (A - A_d)\frac{\partial p}{\partial x_p} \quad (41)$$

it follows that

$$K_p = \alpha_p(A/A_d - 1) \quad (42)$$

From equations (39) and (42) it can be seen that K_p is temperature dependent. The temperature dependency of K_p given by equations (39) and (42) is compared in Fig. 7 with results of an experiment involving a typical engine.

The experiment was performed on an engine-alternator with the displacer locked at its nominal mid-stroke and the alternator used as a motor. Experimental data were obtained by driving the alternator with a variable frequency oscillator, and, by means of electrical measurements, determining the piston resonance at various temperatures. The isothermal prediction can be seen to give a fair approximation for K_p.

With the isothermal approximations for α_p and α_T given by equations (39) and (40), the stability criterion (23) becomes:

$$\frac{m_p}{m_d}\frac{\omega_p}{\omega_d}\left(\frac{\omega_p}{\omega_p + \omega_c}\right)\left(\frac{\omega_p}{\omega_d + \omega_c}\right) \cdot \left[\left(\frac{\omega_c}{\omega_d} - 1\right)^2 + \frac{1}{(4\pi Q_d)^2}\right]^{-1/2} \cdot \left[\left(\frac{\omega_c}{\omega_p} - 1\right)^2 + \frac{1}{(4\pi Q_p)^2}\right]^{-1/2} \cdot \frac{A \cdot A_d}{(A - A_d)^2}\left(1 - \frac{T_c}{T_h} - \frac{A_d}{A}\right) > 1 \quad (43)$$

In practice, $\Delta\omega$ terms and A_d/A are usually small, and the stability criterion is approximately:

$$4\pi^2 \frac{m_p}{m_d}\frac{A_d}{A} Q_d Q_p \left\{1 + \left[4\pi Q_d\left(\frac{\omega_c}{\omega_d} - 1\right)\right]^2\right\}^{-1/2} \cdot \left\{1 + \left[4\pi Q_p\left(\frac{\omega_c}{\omega_p} - 1\right)\right]^2\right\}^{-1/2} \cdot \left(1 - \frac{T_c}{T_h} - \frac{A_d}{A}\right) > 1 \quad (44)$$

It follows from equation (44) that the lowest T_h for onset of oscillation occurs for the special case $\omega_c = \omega_p = \omega_d$, for which the start-up criterion becomes:

$$4\pi^2 \frac{m_p}{m_d}\frac{A_d}{A} Q_d Q_p\left(1 - \frac{T_c}{T_h} - \frac{A_d}{A}\right) > 1 \quad (45)$$

At start-up sliding friction is dominant and determines Q_d and Q_p. If sliding frictional forces F_{sld} and F_{slp} exist against displacer and piston motions respectively and are given by:

$$F_{sld} = -|F_{sld}|\frac{\dot{x}_d}{|\dot{x}_d|}$$

$$F_{slp} = -|F_{slp}|\frac{\dot{x}_p}{|\dot{x}_p|}$$

then at start-up, the quantities Q_d, Q_p are amplitude dependent according to:

$$Q_d = \frac{m_d|X_d|\omega^2}{8|F_{sld}|}$$

$$Q_p = \frac{m_p|X_p|\omega^2}{8|F_{slp}|}$$

and the start-up criterion for equal resonances of the piston and the displacer becomes:

$$\frac{\pi^2}{16}\frac{m_p}{m_d}\frac{A_d}{A}(m_p m_d \omega^4)\frac{|X_d||X_p|}{|F_{sld}||F_{slp}|} \cdot \left(1 - \frac{T_c}{T_h} - \frac{A_d}{A}\right) > 1 \quad (46)$$

which shows that the effect of sliding friction is to impose a minimum product of amplitudes, $|X_d||X_p|$, as a condition for starting. Since equation (46) does not account for flow losses or external loading which become dominant over friction at larger amplitudes, the engine may well start if equation (46) is satisfied but then fail to build up to design amplitudes.

An important conclusion that may be drawn from equations (44) and (46) is that a free-piston Stirling engine can be designed to self-start easily providing that the sliding friction is small and that the small amplitude resonances of the displacer and piston are such that the start-up inequality is satisfied. Practical considerations will often result in the resonances being detuned at rest. For example, the effect of gas spring centering ports, leakage between the gas spring and working gas, and drift of the moving parts under gravity. In these cases the machine will require some input of energy to initiate oscillation.

Once the machine has started, and reached a cyclic steady state, the power follows from equations (29) and (40):

$$P = \frac{\omega}{2}\frac{P_o}{T_c}\frac{T_o}{V_o} A(A - A_d)\left(1 - \frac{T_c}{T_h} - \frac{A_d}{A}\right)|X_d||X_p| \sin\phi \quad (47)$$

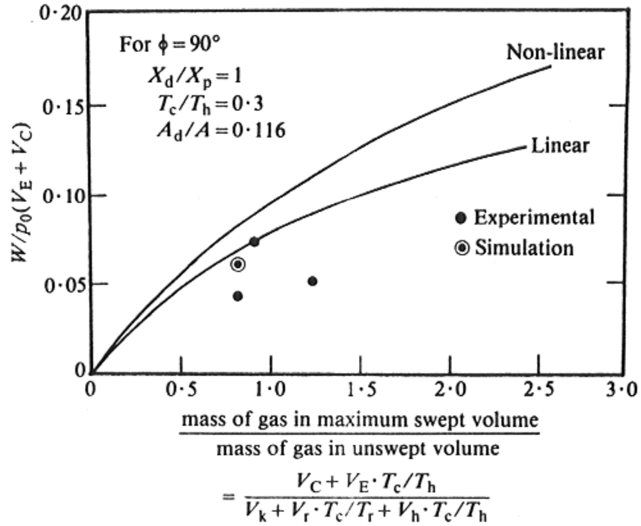

Fig. 8 Comparison between cycle work based on non-linear pressure and linearized pressure

where

$$\frac{V_o}{T_o} = \frac{1}{T_c}\left(\frac{V_c}{2} + V_k\right) + \frac{V_r}{T_r} + \frac{1}{T_h}\left(\frac{V_E}{2} + V_h\right)$$

the amplitude ratio and phase angle having been obtained from equations (26) and (27).

Since power is directly proportional to the mean cycle pressure, Stirling engines usually require pressurization to improve their specific power.

Figure 8 shows the power as predicted by the linear analysis compared to experimental and computer simulation results. Also shown is a solution for power (labelled 'non-linear') assuming isothermal thermodynamics and sinusoidal volume variations (**1, 2, 7**). The 'non-linear' solution accounts for, among other things, the fact that gas spring 'constants' are amplitude dependent.

5 HIGHER DEGREE OF FREEDOM SYSTEMS

In the foregoing analysis the casing motion has been assumed to be zero. However, there are FPSE configurations in which casing motion plays an essential dynamic role. Two such systems will be briefly analysed here, *viz.*, the Harwell thermomechanical generator and the so-called free-cylinder engine. Obviously linear dynamics is applicable to other higher order systems such as the duplex Stirling heat pump and refrigerator, both of which are systems with three degrees of freedom (**4, 5**).

5.1 Harwell thermomechanical generator

This device was originally developed as a long-life (better than ten years) high efficiency electrical generator to be powered by nuclear radioisotopes (**8**). Referring to Fig. 9, the machine consists of a displacer and piston both of which are mechanically sprung to the casing. The load is located between the casing and piston and is indicated by D_{pc}. Casing motion drives the displacer through K_{dc}. Typically, the piston is replaced by a weighted flexing diaphragm.

The casing motions are usually of much smaller amplitude than either the displacer or piston motions.

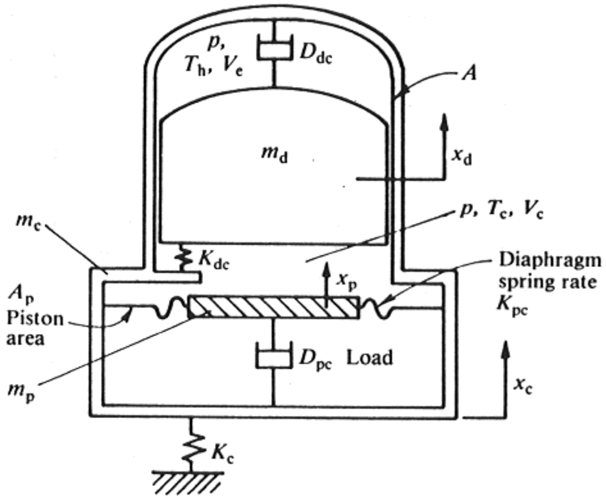

Fig. 9 Harwell thermomechanical generator

Viscous coupling between the casing and displacer or piston may therefore be neglected and the effect of casing motions on the working gas pressure may also be assumed to be negligible. In addition, the viscous coupling between the piston and displacer is ignored with the same reservations as in the previous case. The transformed equations of motion for the displacer and piston may be written:

$$(m_d s^2 + D_{dc} s + K_{dc})\hat{x}_d - K_{dc}\hat{x}_c = 0 \tag{48}$$

$$(m_p s^2 + D_{pc} s + K_{pc} + A\beta_p)\hat{x}_p + A\beta_d \hat{x}_d - K_{pc}\hat{x}_c = 0 \tag{49}$$

where

$$\beta_p = \frac{\partial p}{\partial x_p},\ \beta_d = \frac{\partial p}{\partial x_d}$$

The force exerted by the mounting springs is small compared to the inertia force so that the entire engine is essentially a free body. Thus the transformed equation of motion of the centre of mass may be written:

$$m_c s^2 \hat{x}_c + m_p s^2 \hat{x}_p + m_d s^2 \hat{x}_d = 0$$

or

$$\hat{x}_c = -\frac{m_p}{m_c}\hat{x}_p - \frac{m_d}{m_c}\hat{x}_d \tag{50}$$

Eliminating $\hat{x}_c$ and with the following definitions:

$$\alpha_p = \frac{m_p}{m_c} K_{dc}$$

$$\alpha_T = A\beta_d + K_{pc}\frac{m_d}{m_c}$$

(negative for sufficiently high T_h)

$$K_d = K_{dc}(1 + m_d/m_c)$$

$$K_p = A\beta_p + K_{pc}(1 + m_p/m_c)$$

the following characteristic equation is obtained:

$$T_d(s)T_p(s) - \alpha_p \alpha_T = 0 \tag{51}$$

which is identical in form to equation (12) and therefore the same stability criterion holds, i.e. equation (23).

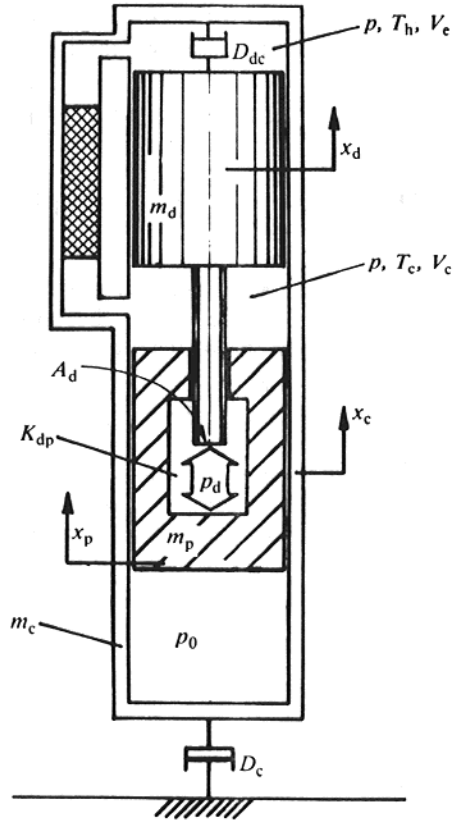

Fig. 10 Free-cylinder engine

Using the isothermal model, α_p and α_T may be evaluated and substituted into equation (23) giving:

$$4\pi^2 Q_d Q_p \frac{m_d}{m_c}\left[\frac{p_o}{K_{dc}}\frac{T_o}{V_o} A A_p\left(\frac{1}{T_c} - \frac{1}{T_h}\right) - \frac{K_{pc}}{K_{dc}}\frac{m_d}{m_c}\right] > 1 \tag{52}$$

for $\omega_p = \omega_d = \omega_c$ and $Q_d \gg 1$, $Q_p \gg 1$.

If the contribution of the diaphragm stiffness to the piston spring rate is small compared to the contribution of the working gas, then for oscillations:

$$4\pi^2 Q_d Q_p \frac{m_p}{m_c}\frac{A}{A_p}(1 - T_c/T_h) > 1 \tag{53}$$

It is interesting to note that since the displacer is mechanically sprung and the piston is a flexing diaphragm, there is no sliding friction or need for centering ports, thus the stability criterion suggests these engines will self-start on application of heat and they in fact do so.

A further observation is that it appears from equation (53) that the instability may be increased by making m_c and A_p small. However, it may be necessary to limit the instability to avoid excessive amplitudes which could have an adverse effect on the life of the diaphragm owing to higher stresses. In this case, the instability may be reduced by reducing Q_d and Q_p or by increasing the casing mass and/or the piston area.

5.2 Free-cylinder engine

The free-cylinder Stirling engine offers a means by which mechanical power extraction devices (e.g., a water pump) may be coupled externally to a pressurized, sealed engine. It uses a relatively heavy piston so that useful forces and motions are transferred to the engine casing (**9**). Linear dynamics predicts that, unlike the free-piston engine, it has the ability to start at any value of load (D_c in Fig. 10).

The linear analysis summarized below shows that the free-cylinder engine behaves essentially like a free-piston engine for which ω_p and Q_p vary with load damping D_c.

With the definitions:

$$\beta_p = \frac{\partial p}{\partial x_p}, \quad \beta_d = \frac{\partial p}{\partial x_d}, \quad \beta_c = \frac{\partial p}{\partial x_c}$$

$$K_p = (A - A_d)\beta_p + K_{dp}$$

$$K_d = (A_d \beta_d + K_{dp})$$

(positive for K_{dp} sufficiently high)

$$\alpha_T = -(A - A_d)\beta_d - K_{dp}$$

(positive for T_h sufficiently high)

$$\alpha_{pd} = A_d \beta_p - K_{dp}$$

(positive for $A_d \beta_p$ sufficiently high)

where, again, A is the cylinder cross-sectional area and A_d is the displacer rod cross-sectional area. The Laplace transformed equations of motion of displacer, piston and centre of mass respectively, linearized about a point for which $p = p_o$, are:

$$(m_d s^2 + D_d s + K_d)\hat{x}_d + \alpha_{pd}\hat{x}_p + A_d \beta_c \hat{x}_c = 0 \tag{54}$$

$$(m_p s^2 + K_p)\hat{x}_p + (A - A_d)\beta_c \hat{x}_c - \alpha_T \hat{x}_d = 0 \tag{55}$$

$$\hat{x}_c = -\frac{m_p s \hat{x}_p}{m_c s + D_c} \tag{56}$$

Some terms that have little influence on the dynamics in practical cases have been dropped.

Using the equation of centre of mass motion to eliminate $\hat{x}_c$, and with the further definitions:

$$K_c = -(A - A_d)\beta_c \frac{m_p}{m_c} \quad \text{(positive quantity)}$$

$$\alpha_{cd} = -A_d \beta_c \frac{m_p}{m_c} \quad \text{(positive quantity)}$$

the transformed equations of displacer and piston motion become:

$$(m_d s^2 + D_d s + K_d)\hat{x}_d + \left[\alpha_{pd} + \alpha_{cd}\left(\frac{s}{s + D_c/m_c}\right)\right]\hat{x}_p = 0 \tag{57}$$

$$\alpha_T \hat{x}_d - \left[m_p s^2 + K_p + K_c\left(\frac{s}{s + D_c/m_c}\right)\right]\hat{x}_p = 0 \tag{58}$$

Two limiting cases can be distinguished. First, for $D_c = \infty$ (fixed casing), equations (57) and (58) reduce to:

$$(m_d s^2 + D_d s + K_d)\hat{x}_d + \alpha_{pd}\hat{x}_p = 0 \tag{59}$$

$$\alpha_T \hat{x}_d - (m_p s^2 + K_p)\hat{x}_p = 0 \tag{60}$$

Equations (59) and (60) are the equations of a free-piston engine having infinite piston Q and a piston resonance frequency ω_{pi} given by

$$\omega_{pi} = \left(\frac{K_p}{m_p}\right)^{1/2} \tag{61}$$

If $D_c = 0$, equations (57) and (58) reduce to:

$$(m_d s^2 + D_d s + K_d)\hat{x}_d + (\alpha_{pd} + \alpha_{cd})\hat{x}_p = 0 \tag{62}$$

$$\alpha_T \hat{x}_d - (m_p s^2 + K_p + K_c)\hat{x}_p = 0 \tag{63}$$

Equations (62) and (63) are again the equations of motion of a free-piston Stirling engine having infinite piston Q and, in this case, a piston resonance frequency, ω_{po}, given by:

$$\omega_{po} = \left(\frac{K_p + K_c}{m_p}\right)^{1/2} \tag{64}$$

Comparison of equations (59) and (62) shows that the coupling constant relating piston movement to driving force on the displacer increases from α_{pd} for a locked casing to $(\alpha_{pd} + \alpha_{cd})$ for a free casing. This is because of casing motion in opposition to piston motion and has dynamic consequences which will be discussed later.

As previously, the general characteristic equation of the system is found by setting the determinant of the coefficients of equations (57) and (58) equal to zero. The characteristic equation is:

$$\frac{m_p m_d[s(s^2 + \omega_{po}^2) + (D_c/m_c)(s^2 + \omega_{pi}^2)][s^2 + \omega_d s/2\pi Q_d + \omega_d^2]}{s + D_c \alpha_{pd}/[m_c(\alpha_{pd} + \alpha_{cd})]} + \alpha_T(\alpha_{pd} + \alpha_{cd}) = 0 \tag{65}$$

From equation (65) it is evident that a single LHP pole of the first term of equation (65) exists at:

$$s = -\frac{D_c \alpha_{pd}}{m_c(\alpha_{pd} + \alpha_{cd})}$$

There are five zeros since the numerator is fifth order. Two of these are roots of:

$$s^2 + \frac{\omega_d}{2\pi Q_d} s + \omega_d^2 = 0 \tag{66}$$

For $Q_d \gg 1$, the roots of equation (66) are $s = -\omega_d/4\pi Q_d \pm j\omega_d$. The remaining three zeros are roots of:

$$s(s^2 + \omega_{po}^2) + \frac{D_c}{m_c}(s^2 + \omega_{pi}^2) = 0 \tag{67}$$

If $D_c = 0$, the roots of equation (67) are $s = 0$ and $s = \pm j\omega_{po}$. As $D_c = \infty$, the roots of equations (67) are $s = -D_c/m_c$ and $s = \pm j\omega_{pi}$.

For finite values of D_c, root locus techniques can be used to give general information on the roots of equation (67). It can be shown that as D_c increases from zero, two roots depart from $\pm j\omega_{po}$ into the left half plane, in a direction parallel to the real axis, and, as $D_c \to \infty$, these two roots approach $\pm j\omega_{pi}$ from a direction parallel to the real axis. For $m_p/m_c \gg 1$, it can be shown that the loci of these two roots are semicircles in the left half plane. Root locus methods also show that the root at $s = 0$ moves to the left on the real axis as D_c increases, and approaches $-D_c/m_c$ as $D_c \to \infty$.

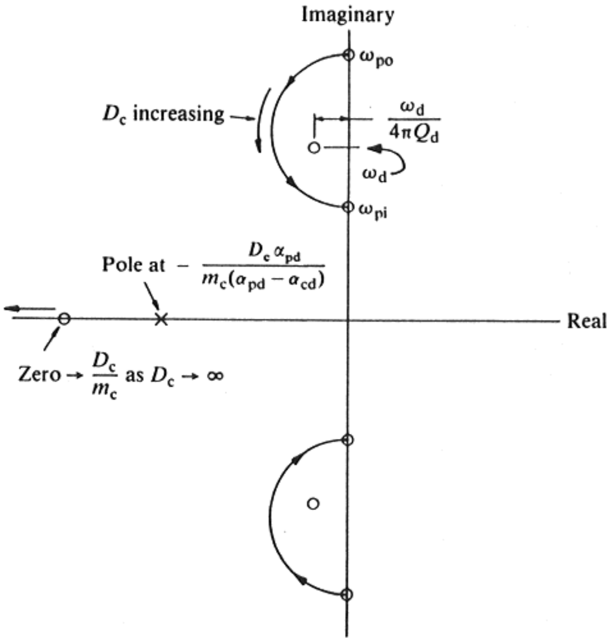

Fig. 11 Loci of poles and zeros of free-cylinder engine

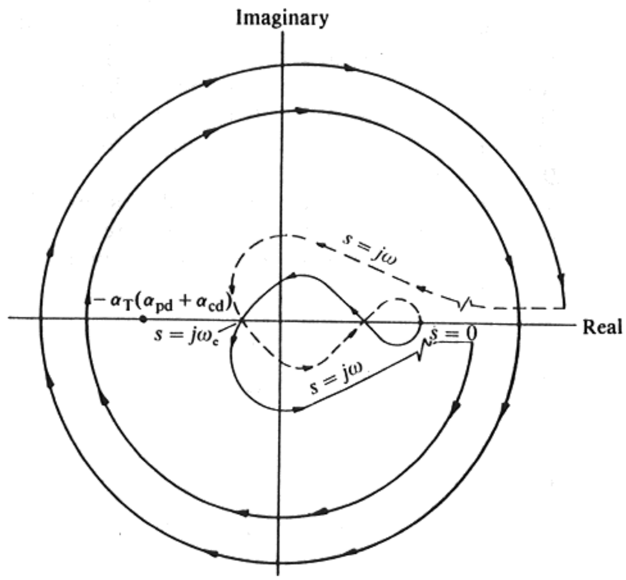

Fig. 12 Location of $\alpha_T(\alpha_{po} + \alpha_{cd})$ for two RHP roots

Figure 11 shows the loci of the poles and zeros of the first term of equation (65) for a case where ω_d lies between ω_{po} and ω_{pi}.

With the help of Fig. 11, a map of the first term of equation (65) as s traverses the Bromwich contour can be sketched, as shown in Fig. 12 for a typical value of D_c.

If the first term of equation (65) is expressed in magnitude-angle form $M \angle \theta$ then ω_c in Fig. 12 is the frequency at which $\theta = \pi$. If

$$M(\omega_c) < \alpha_T(\alpha_{pd} + \alpha_{cd}) \quad (68)$$

then there are two clockwise encirclements of the point $-\alpha_T(\alpha_{pd} + \alpha_{cd})$ by the map, otherwise there are no net encirclements (two clockwise, two counterclockwise). Thus equation (68) is a necessary condition for oscillation. For Q_d high, $\omega_c \approx \omega_d$ for finite D_c. Then, since $M(\omega_c)$ is proportional to the product of phasors joining the point $s = j\omega_c$ to the zeros of the first term of equation (65), it is clear from Fig. 11 that Q_d is critical in determining whether oscillation will occur over the entire range of D_c. Also important is the value of ω_d relative to ω_{po} and ω_{pi}. To minimize the maximum value of $M(\omega_c)$ over the entire range of D_c, ω_d should evidently lie between ω_{po} and ω_{pi}. Since the coupling constant between piston movement and driving force on the displacer is higher for the free casing than for the fixed casing, instability is easier to achieve for D_c near zero than for high values of D_c. Thus, ω_d should be closer to ω_{pi} than ω_{po} in order to achieve approximately the same value of α_T for instability at all values of D_c.

6 CONCLUSIONS

By the application of linear dynamics to free-piston Stirling engines the following has been shown:

1. Existence of a stability criterion which relates mechanical dynamics and thermodynamics and shows that there is a minimum hot end temperature for which oscillation may be expected.
2. That there is only one mode of oscillation for each of the engines treated here, i.e., only one pair of RHP roots.
3. Frequency is generally load dependent but the engine may be configured to operate at essentially constant frequency for wide changes in load.
4. Once the machine begins to oscillate, non-linearities must act to prevent a runaway condition.
5. The presence of sliding friction imposes a condition of a minimum amplitude product, $|X_d||X_p|$, for starting. In the absence of sliding friction, a properly configured engine will self-start at or above a minimum starting temperature.
6. Arranging $\omega_d = \omega_p$ allows the engine to start at a lower hot end temperature, and maximizes the power for a fixed geometry.
7. The closed-form results from linear dynamics and simple isothermal thermodynamics offer a quick and convenient method for preliminary engine sizing.
8. The casing plays an essential part in the operation of two higher degree of freedom engines. In particular, for the Harwell machine the casing reaction to piston motion is the source of feedback to excite the displacer. The free-cylinder engine employs the motion of the cylinder to deliver its power. This machine has the unique characteristic in that, if properly designed, it will continue to oscillate at any load from zero to infinity and will also self-start under any load.

More generally, linear dynamics provides direct means for understanding the behaviour of a free-piston engine over the complete operating parameter set and shows the influence of engine geometry on this behaviour. Practical issues such as sliding friction, the presence of centering ports or the effect of drift under gravity may also be included. By virtue of being able to address the broad spectrum of operating conditions and design parameters, the analysis therefore offers a clear qualitative appreciation of these engines' idiosyncracies too.

REFERENCES

1 **Walker, G.** *Stirling engines.* 1980 (Oxford University Press, Oxford).
2 **Reader, G. T.** and **Hooper, C.** *Stirling engines,* 1983 (E. and F. N. Spon, London).
3 **Beale, W. T.** Free piston Stirling engines—some model tests and simulations. SAE paper No. 690230, Jan. 1969.
4 **Penswick, L. B.** and **Urieli, I.** Duplex Stirling Machines. *Proc. 19th IECEC,* San Francisco, California, Aug. 1984.
5 **Berchowitz, D. M.** The design, development and performance of a duplex Stirling natural gas liquifier. *Proc. 17th IECEC,* paper No. 829296, Los Angeles, California, Aug. 1982.
6 **Thomason, J. G.** *Linear feedback analysis,* 1956, 136–143 (McGraw-Hill, New York).
7 **Urieli, I.** and **Berchowitz, D. M.** *Stirling cycle engine analysis,* 1984 (Adam Hilger, Bristol).
8 **Cooke-Yarborough, E. H.,** *et al.* Harwell thermomechanical generator. *Proc. 9th IECEC,* paper No. 749156, San Francisco, Aug. 1974.
9 **Beale, W. T.,** *et al.* Free cylinder Stirling engines for solar-powered water pumps. ASME Paper No. 71-WA/Sol-11, Aug. 1971.